

Article

## Synthesis and Characterization of Hybrid Materials Consisting of *n*-octadecyltriethoxysilane by Using *n*-Hexadecylamine as Surfactant and Q<sup>0</sup> and T<sup>0</sup> Cross-Linkers

Ismail Warad <sup>1,\*</sup>, Omar Abd-Elkader H <sup>2,3</sup>, Saud Al-Resayes <sup>1</sup>, Ahmad Husein <sup>4</sup>,  
Mohammed Al-Nuri <sup>4</sup>, Ahmed Boshala <sup>5</sup>, Nabil Al-Zaqri <sup>1</sup> and Taibi Ben Hadda <sup>6</sup>

<sup>1</sup> Department of Chemistry, Science College, King Saud University, P.O. Box 2455, Riyadh 11451, Saudi Arabia; E-Mails: resayes@ksu.edu.sa (S.A.-R.); nabil\_alzaqri@yahoo.com (N.A.-Z.)

<sup>2</sup> Electron Microscope Unit, Zoology Department, College of Science, King Saud University, Riyadh 11451, Kingdom of Saudi Arabia; E-Mail: omabelkader7@yahoo.com

<sup>3</sup> Electron Microscope & Thin Films Department, Physics Division, National Research Center, Dokki 12622, Cairo, Egypt

<sup>4</sup> Department of Chemistry, Science College, AN-Najah National University, P.O. Box 7, Nablus 00972, Palestine Territories; E-Mails: hamaydah2500@yahoo.com (A.H.); mabnuri@yahoo.com (M.A.-N.)

<sup>5</sup> Chemistry Department, Faculty of Science, Benghazi University, P. O. Box 1308, Benghazi, 22385, Libya; E-Mail: ahmedboshala@yahoo.co.uk

<sup>6</sup> Materials Chemistry Laboratory, Faculty of Sciences, University of Mohammed Premier, Oujda-60000, Morocco; E-Mail: taibi.ben.hadda@gmail.com

\* Author to whom correspondence should be addressed; E-Mail: warad@ksu.edu.sa;  
Tel.: +96-61-4675992; Fax: +96-61-4675992.

Received: 12 April 2012; in revised form: 3 May 2012 / Accepted: 10 May 2012 /

Published: 21 May 2012

---

**Abstract:** Novel hybrid xerogel materials were synthesized by a sol-gel procedure. *n*-octadecyltriethoxysilane was co-condensed with and without different cross-linkers using Q<sup>0</sup> and T<sup>0</sup> mono-functionalized organosilanes in the presence of *n*-hexadecylamine with different hydroxyl silica functional groups at the surface. These polymer networks have shown new properties, for example, a high degree of cross-linking and hydrolysis. Two different synthesis steps were carried out: simple self-assembly followed by sol-gel transition and precipitation of homogenous sols. Due to the lack of solubility of these

materials, the compositions of the new materials were determined by infrared spectroscopy,  $^{13}\text{C}$  and  $^{29}\text{Si}$  CP/MAS NMR spectroscopy and scanning electron microscopy.

**Keywords:** sol-gel; solid state NMR; cross-linkers; stationary phases

---

## 1. Introduction

Alkyl stationary phases are widely used in liquid chromatography (LC). Much effort has been made to prepare and describe the chromatographic properties [1]. In this field, the application of stationary phases based on silica gel is very popular. For the successful employment of silica, it is of great importance that the silica beads show a narrow particle size distribution and spherical shape. Most HPLC separations are carried out under reversed phase (RP) conditions [2]. The surface modification of well-defined silica beads with T-silyl functionalized organic systems is the major route to create phases for reversed-phase liquid chromatography (RPLC) [3–5]. All the RP prepared by the different conventional methods (solution or surface polymerized modification and monomeric synthesis) mentioned above do not exhibit complete cross-linked **T** and **Q** units. For long-term stability of stationary phases it is very important to prepare one with a high degree of cross-linked ligands. This may be achieved using the sol-gel process.

Sol-gel processing of polysiloxanes to prepare hybrid inorganic-organic materials (HIOM) [6–9] is quite a promising technique in field of chromatography [10,11]. It has been widely investigated to prepare potential matrices for reporter molecules in chemistry sensors [12]. More recently, such materials have also received attention as catalyst supports, enzymes and catalytically active transitions metal complexes [13].

Recently, many investigations were extended to nanostructure mesoporous silicas which are based on inorganic-organic hybrid polymers [14–19]. These materials possess extremely high surface areas and accessible pores. Moreover, the pore size can be tuned with different sizes in the nanometer range by choosing template systems or with a co-solvent [15]. For the generation of stationary phases, T-functionalized silanes of the type  $\text{F}_n\text{-Si(OR)}_3$  were sol-gel processed with and without co-condensation agents, which play an important role in controlling the density and the distance of the reactive centers; in general  $\text{F}_n$  represents either alkyl spacer alone or end by a metal complex [20]. These reactive centers are distributed across the entire carrier matrix and play an important role in catalysis [21–38].

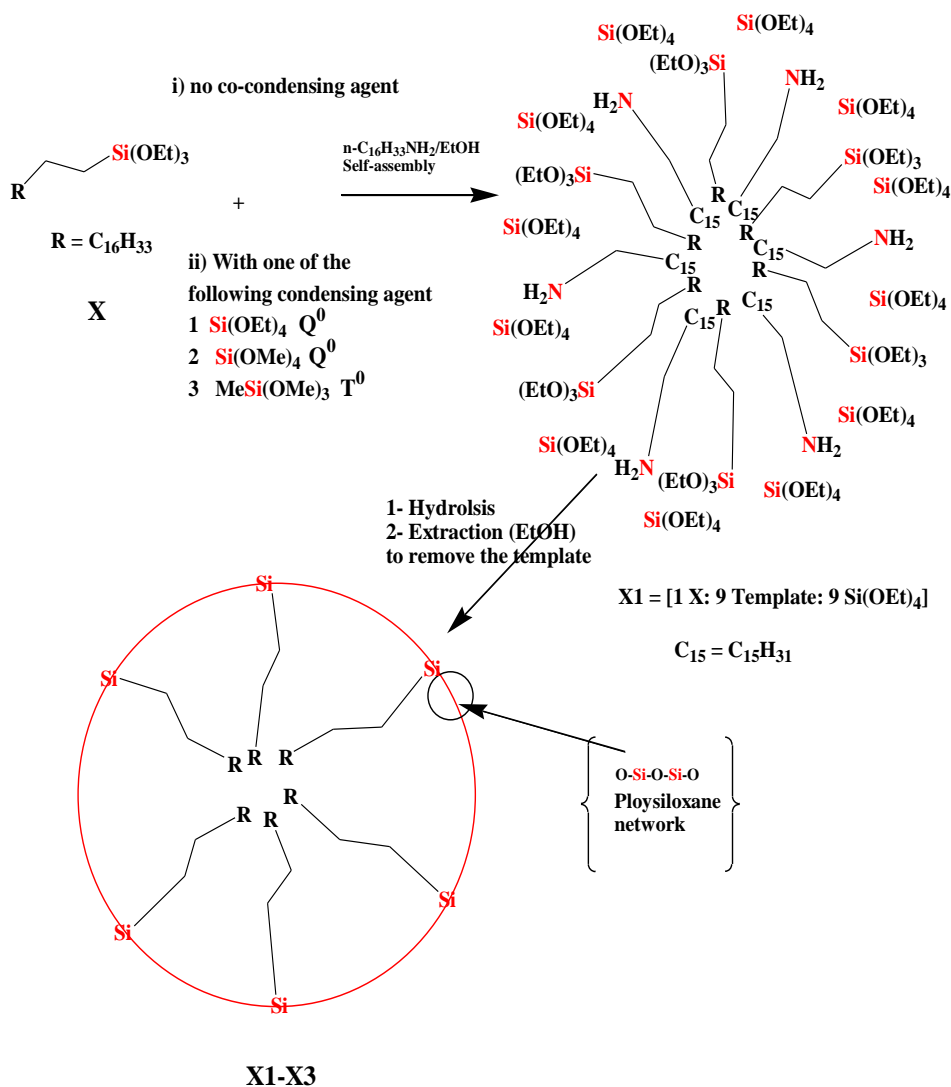
In this work, hybrid materials were synthesized by a simple one-step self assembly followed by co-condensation of different silane cross-linkers with *n*-octadecyltrialkoxysilane as the chromatographic selector in the presence of *n*-hexadecylamine surfactant. Application of different alkoxysilane co-condensation agents, such as  $\text{Si(OEt)}_4$ ,  $\text{Si(OMe)}_4$  (**Q**<sup>0</sup>) and  $\text{MeSi(OMe)}_3$  (**T**<sup>0</sup>) during the sol-gel processes enable the building of polymer frameworks with different hydroxyl silica functional groups and new properties compared to surface modified silica gel.

## 2. Results and Discussion

### 2.1. Sol-Gel Processing

The properties of the sol-gel processed products strongly depend on the reaction conditions, such as type of solvent, temperature, time, catalysts, concentration of the monomers and type of the cross-linkers [9,10]. To ensure comparable results, uniform reaction conditions throughout hydrolysis and the sol-gel transition have been maintained. Alcohol is necessary to homogenize the reaction mixture. All poly-condensations were performed in a mixture of ethanol with a certain amount of water as catalyst for the sol-gel process (see Experimental section). Long alkyl chains commonly used for liquid chromatography were introduced by using the  $\text{CH}_3(\text{CH}_2)_{17}\text{Si}(\text{OEt})_3$ , *n*-octadecyltriethoxysilane (**X**), in the presence of *n*-hexadecylamine as template, which concomitantly serves as material to allow mesoporous hybrid compounds. During the sol-gel process, a fixed ratio of **X**, template and co-condensation agents [1:9:9], respectively, were used. Several types of co-condensation agents used, such as  $\text{Si}(\text{OEt})_4$  (TEOS),  $\text{Si}(\text{OMe})_4$  (TMOS) and  $\text{MeSi}(\text{OMe})_3$ , are shown in Scheme 1.

**Scheme 1.** Synthesis of xerogels **X0–X3**: Self-assembly followed by sol-gel process at room temperature using several cross-linkers and the amine as template.



After sol-gel processing, the amine was removed from the mixture by Soxhlet extraction with ethanol. Four xerogels (**X0–X3**) were collected and are illustrated in Table 1.

**Table 1.** Sol-gel processes, yields and labeling of the materials.

No.	Xerogel	Cross-Linkers Types	Yield %	Silyl Fragments
1	<b>X0</b>	-	60.0	<b>T<sup>2</sup></b> and <b>T<sup>3</sup></b>
2	<b>X1</b>	Si(OEt) <sub>4</sub>	77.6	<b>T<sup>2</sup></b> , <b>T<sup>3</sup></b> , <b>Q<sup>3</sup></b> and <b>Q<sup>4</sup></b>
3	<b>X2</b>	Si(OMe) <sub>4</sub>	64.5	<b>T<sup>2</sup></b> , <b>T<sup>3</sup></b> , <b>Q<sup>3</sup></b> and <b>Q<sup>4</sup></b>
4	<b>X3</b>	MeSi(OMe) <sub>3</sub>	72.5	<b>T<sup>2</sup></b> and <b>T<sup>3</sup></b>

Two kinds of stationary phases were obtained: (i) xerogels **X0** were synthesized by co-condensation of **X** and template with zero concentration (**0**) of cross-linker, and (ii) xerogels **X1–X3** were synthesized by co-condensation of **X**, template with monofunctional **Q<sup>0</sup>** and **T<sup>0</sup>** cross-linkers such as Si(OEt)<sub>4</sub>, Si(OMe)<sub>4</sub> and MeSi(OMe)<sub>3</sub>, respectively.

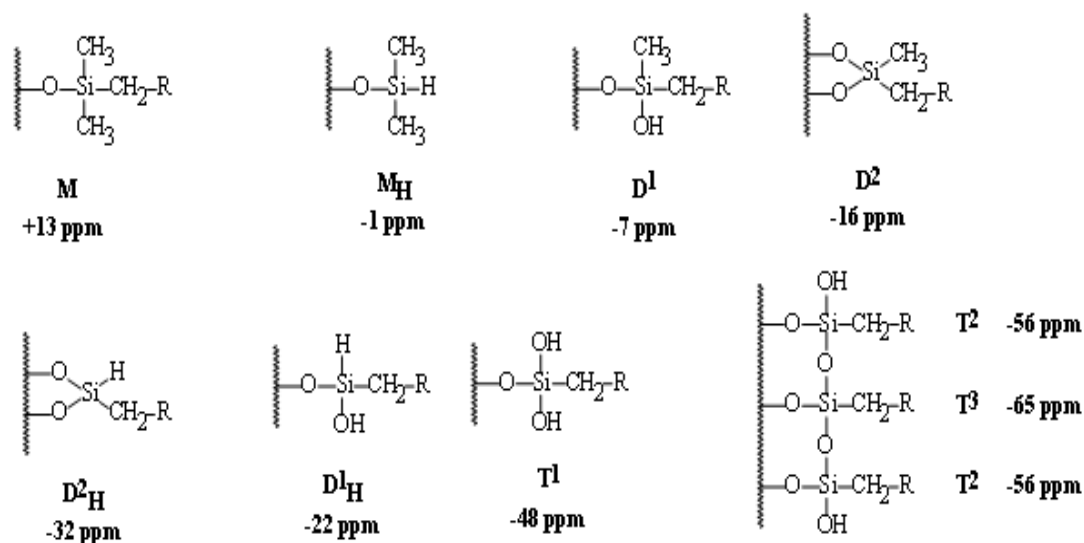
## 2.2. Solid-State NMR Spectroscopic Investigations

Due to cross-linking effects, the solubility of the polymeric materials **X0–X3** is rather limited. Therefore, solid-state NMR spectroscopy was used as a powerful technique for their characterization.

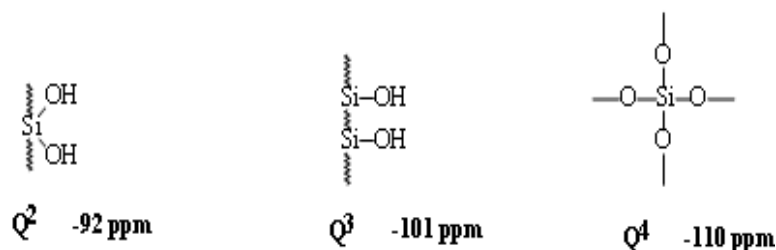
### <sup>29</sup>Si CP/MAS NMR spectroscopy

Silane functionality and bonding chemistry can easily be determined by <sup>29</sup>Si CP/MAS NMR spectroscopy. The universal chemical shift and symbols for these <sup>29</sup>Si function groups are collected in Scheme 2.

**Scheme 2.** The universal <sup>29</sup>Si chemical shifts, symbols and orders of silyl species.



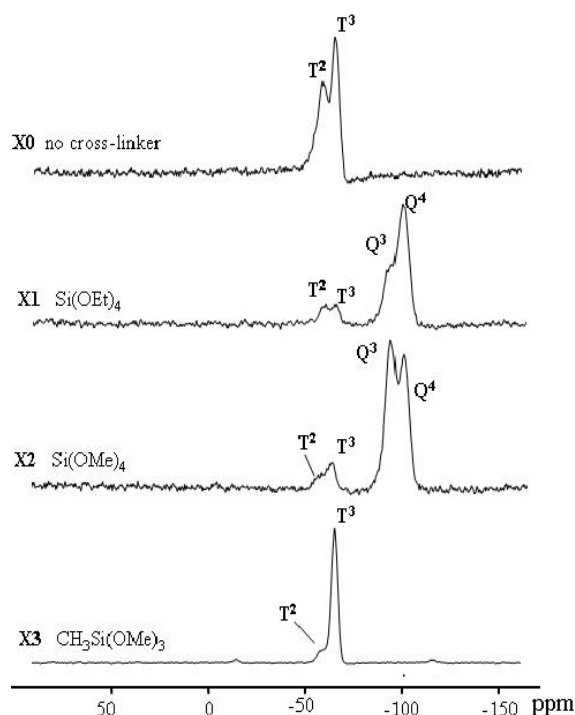
## Scheme 2. Cont.



The average chemical shifts for  $\text{T}^2$  ( $\delta = -58.8$ ), and  $\text{T}^3$  ( $\delta = -65.1$ ),  $\text{Q}^3$  ( $\delta = -101.9$ ),  $\text{Q}^4$  ( $\delta = -109.5$ ) species are significantly changed by the incorporation of the different types of co-condensation agents and are in agreement with values reported in the literature for comparable systems [37]. Since all silicon atoms are in direct proximity of protons the Hartmann–Hahn [29–33] match could efficiently be achieved.

The signal assignment of silyl fragments can be summarized as follows: a higher degree of cross-linking of silicon species and/or an increase of oxygen neighbors leads to an upfield shift in NMR spectra. Difunctional species ( $\text{D}_n$ ) appear in the region of  $-7$  to  $-20$  ppm, tri-functional species ( $\text{T}_n$ ) from  $-49$  to  $-66$  ppm, and signals from the native silica ( $\text{Q}_n$ ) from  $-91$  to  $-110$  ppm. The high condensation degrees which were obtained through the sol-gel processes and monitored by  $^{29}\text{Si}$  NMR is mainly resonated to the employment of  $\text{T}^2$ ,  $\text{T}^3$ ,  $\text{Q}^3$  and  $\text{Q}^4$  as cross-linkers [28–35].

**Figure 1.**  $^{29}\text{Si}$  CP/MAS NMR spectra of **X0–X3** materials which were prepared by using  $\text{Si}(\text{OEt})_4$ ,  $\text{Si}(\text{OMe})_4$  and  $\text{MeSi}(\text{OMe})_3$  as cross-linkers.



All the spectra of xerogels (**X0–X3**) show signals for substructures corresponding to **T** and **Q** functions only, the **D** or **M** silyl fragment has not been observed, as seen in Figure 1. **X0–X3** showed **T** silyl fragment only in general 3 order predominated over 2, which supports the full cross-linked

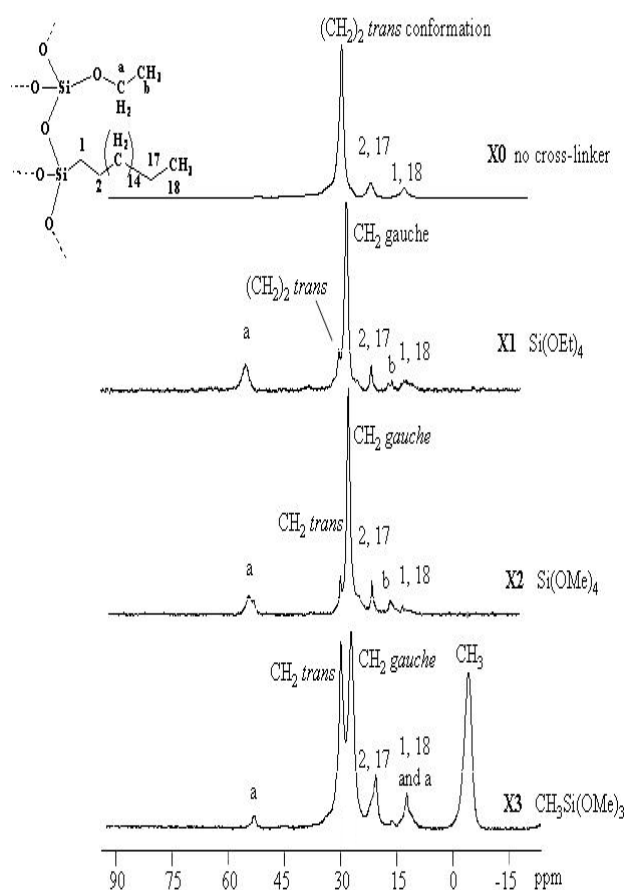
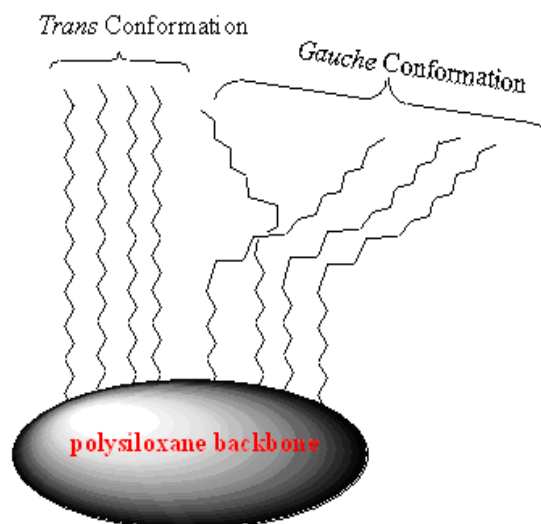
organosiloxane species, demonstrating the incorporation of the function groups within the framework walls of the mesostructures.  $T^2$  silyl fragment indicated that one Si-OH function group of the sector or cross-linkers  $MeSi(OMe)_3$  was not incorporated in the sol-gel process. **X0** and **X3** revealed only T silyl fragment, and this was expected since no Q co-condensation agents were used. **X1** and **X2** showed both T and Q with 2 and 3 order, because both the sector T silyl fragment and Q silyl fragment of the co-condensation agents were investigated in the sol-gel process; Q predominated over T due to the concentrations used [9:1] respectively. The respective NMR spectra of the different materials' phases and the native silica are shown in Figure 1.

### 2.3. $^{13}C$ CP/MAS NMR Spectroscopy

More detailed information on bonded phase architecture was obtained from the  $^{13}C$  CP/MAS NMR spectra of the supported matrices **X0–X3**, and the corresponding signal assignments are summarized in Figure 2. Characteristic peaks at approximately  $\delta = 14.0$  ppm are assigned to the carbon atom of  $CH_3$  and the carbon atom of the silicon adjacent methyl groups ( $SiCH_2$ ) in the Si–O–Si substructure  $\delta = 22.8$  ppm is assigned to  $CH_2CH_3$  and  $SiCH_2CH_2$  are significant for all the stationary phases. Weak signals of  $^{13}C$  were assigned to residual Si–OR (R = Me or Et) functionalities at around  $\delta = 17.0$  and 57.9 ppm, attributed to non-hydrolyzed EtO (**X1**) or MeO (**X2** and **X3**) silica functional groups, which point to a high degree of hydrolysis compared to the literature [7,9].  $\delta = -3.6$  ppm is assigned to SiMe in case of using  $MeSi(OMe)_3$ . The NMR investigation of such stationary bonded phases exhibits two signals for the main chain methylene carbons at 30.0 and 32.2 ppm (*gauche/trans* conformations, respectively) as shown in Figure 2 [5].

The samples **X1**, **X2** and **X3** show two peaks related to the main chain  $(CH_2)_{14}$  at 30.0 and 32.0 ppm which represent two different conformations of the alkyl chain. The signal at 32.8 ppm characterizes *trans* conformations, and the signal at 30.0 ppm reveals the existence of *gauche* conformations. The effect of different motilities is only visible in the  $^{13}C$  CP/MAS NMR spectra of the xerogels containing alkyl chains with 18 carbon atoms at least; the alkyl chain order is found to increase with increasing chain length from  $C_{18}$  to  $C_{34}$  [36].

The NMR investigation of  $C_{18}$  bonded phases here exhibits only one signal for the main chain: methylene carbons at 32.8 belong to the *trans* conformation when no co-condensation agent was investigated (**X0**). When TESO or TMSO ( $Q^0$ ) was introduced to the sol-gel, the presence of the Me-Si function group in the cross-linker plays a key role in the conformation; the *trans* conformation was encouraged. The main reason of such a phenomenon is not yet clear, it could be related to the un-hydrolysis Me-Si steric factor of remaining Me on the **X3** polysiloxane surface affecting the  $C_{18}$  chain not to bend away to form a *gauche* conformation, thus enhancing the C–H Wander Val forces to form sort of stabilizing straight line chains as in Scheme 3. This proposal is compatible with the decrease in the *trans* conformation at the expense of the alternative *gauche* conformation increasing upon increasing the temperature [9,28–30].

**Figure 2.**  $^{13}\text{C}$  CP/MAS NMR spectra of X0-X3 materials.**Scheme 3.** Schematic illustration of *trans* and *gauche* alkyl chain arrangements.

Here we report a new method at room temperature to control the *gauche/trans* conformation ratio of the alkyl chains in the stationary phase by using fixed concentrations of several type of  $\text{T}^0$  and  $\text{Q}^0$  cross-linkers.

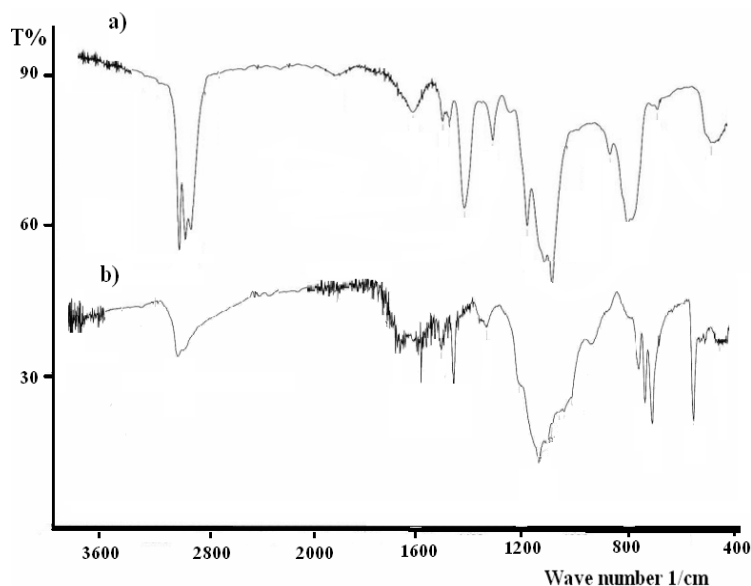
#### 2.4. IR Investigations

The IR spectra of the desired materials, **X0**, **X1**, **X2** and **X3** in particular, show several peaks that are attributed to stretching and bending. The broad intensive stretching vibrations at  $2980\text{--}2840\text{ cm}^{-1}$  and bending vibrations at  $1150\text{--}950\text{ cm}^{-1}$  belonging to ( $\nu_{\text{CH}}$ ) of the  $\text{SiCH}_2(\text{CH}_2)_{16}\text{CH}_3$  functional groups were the main IR active functional groups. A typical example of the IR behavior of **X3** is illustrated in Figure 3b.

In order to confirm the full sol-gel reaction, the structural vibration behaviors of these compounds against the infrared spectra of **X** as the starting material and **X3** as xerogel before and after the sol-gel processes were investigated and compared, such as the typical examples in Figure 3.

The broad intensive stretching vibrations at  $2980\text{--}2840\text{ cm}^{-1}$  of ( $\nu_{\text{CH}}$ ) belong to the  $\text{SiOCH}_2\text{CH}_3$  functional groups of **X** starting material as in Figure 3a totally disappeared after the sol-gel process to prepare the complex **X3** as seen in Figure 3b, which strongly confirms the completeness of the sol-gel process formation.

**Figure 3.** Infra-red spectra (a and b) of **X** and **X3**, before and after sol-gel, respectively.

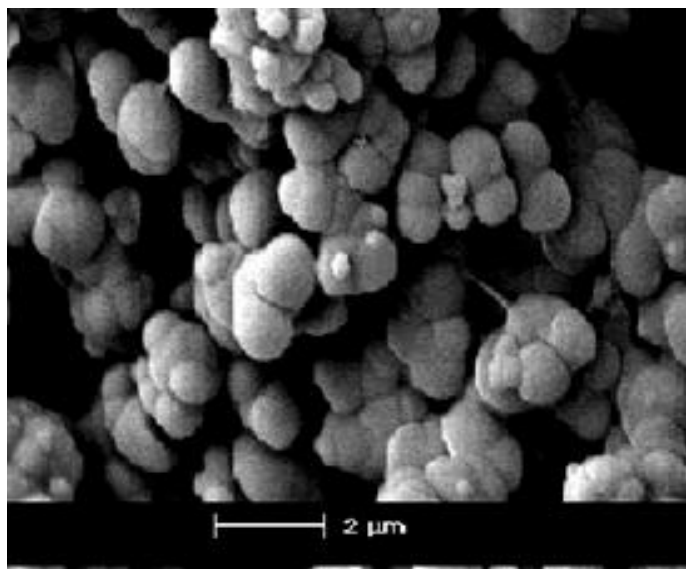


#### 2.5. Surface Structure of the Materials

The surface area data (BET) of such materials determined by the sol-gel procedure was found to equal  $1000\text{--}1500\text{ m}^2/\text{g}$ ,  $0.5\text{--}1.3\text{ cm}^3/\text{g}$  pore volume, and  $13\text{--}20\text{ \AA}$  pore size [37].

SEM micrographs of the **X2** and **X3** powder are given in Figure 4. Morphological features of the samples show the difference between spherical shapes, colloidal and porous structure and irregular particles mainly with the size  $0.5\text{--}2\text{ }\mu\text{m}$ . All powders consisted of hard sub micrometer agglomerates, which are composed of fine crystallites. Generally, these agglomerate particles are hard to break down even with a long ultra-sonication time.



**Figure 4.** Scanning electron micrograph (SEM) of X2.

### 3. Experimental

#### 3.1. General Methods

All reactions were carried out in an inert atmosphere (argon) by using standard high vacuum and Schlenk-line techniques unless otherwise noted. *n*-octadecyltriethoxysilane was purchased from ABCR GmbH, Germany. Prior to use, *n*-hexane and Et<sub>2</sub>O were distilled from both LiAlH<sub>4</sub> and sodium/benzophenone, respectively. All other chemicals were obtained from Merck KGaA Darmstadt, Germany, and were used without further purification.

#### 3.2. Method of Characterization

<sup>13</sup>C CP/MAS NMR spectra were recorded on a Bruker ASX 300 spectrometer (Bruker GmbH, Rheinstetten, Germany) at a spinning rate of 4000 Hz with 7 mm double bearing rotors of ZrO<sub>2</sub> and proton of 90° pulse length and 7 μs was used. The contact time and delay time were 3 ms and 3 s, respectively with the line broadening of 30 Hz.

<sup>29</sup>Si CP/MAS NMR spectra were also collected on a Bruker ASX 300 NMR spectrometer. Representative samples of 200–250 mg were spun at 3500 Hz using 7 mm double bearing ZrO<sub>2</sub> rotors. The spectra were obtained with a cross-polarization contact time of 5 ms. The pulse interval time was 1 s. Typically, 1.5 k FIDs with an acquisition time of 30 ms were accumulated in 1 kb data points and zero-filling to 8 kb prior to Fourier transformation. Line broadening of 30 Hz and respective spectral width were found for all spectra at about 20 kHz.

Scanning electron microscopy was performed on a JEOL JSM-6380 LA scanning electron microscope (SEM).

#### 3.3. General Procedure for the Sol-Gel Processes

$2.2 \times 10^{-2}$  mmol of *n*-hexadecylamine (template) in 50 mL of absolute ethanol was completely dissolved. The addition of  $2.4 \times 10^{-3}$  mmol of *n*-octadecyltriethoxysilane (selector) to the template

solution and stirring for 3 h is an important step for self-assembly.  $2.2 \times 10^{-2}$  mmol of the corresponding cross-linker was added and stirred for 10 h, at 35 °C with a molar substrate [1:9:9] [Selector:Template:Cross-linker] respectively. An excess (5 g) of distilled water was added drop wise to a stirred solution. This mixture was stirred for 24 h at room temperature until a gel was formed, then the solvent was removed by reducing the pressure. For the removal of *n*-hexadecylamine the crude xerogels were placed in a Soxhlet extractor containing 300 mL ethanol and the mixture was refluxed for 3 days. Subsequently the gels were washed three times with *n*-hexane and ether (100 mL) respectively, and dried under vacuum for 12 h.

**Polysiloxanyloctane (X0).** A mixture of 1 g ( $2.4 \times 10^{-3}$  mmol) of *n*-octyltrimethoxysilane and 5.2 g ( $2.2 \times 10^{-2}$  mmol) *n*-hexadecylamine were sol-gel processed in ethanol and water to yield a colorless swollen gel. After purification and drying 0.6 g of white powder was formed.  $^{13}\text{C}$  CP/MAS NMR  $\delta = 14.0$  (SiCH<sub>2</sub> and CH<sub>3</sub>), 22.8 (SiCH<sub>2</sub>CH<sub>2</sub> and CH<sub>2</sub>CH<sub>3</sub>), 32.8 [(CH<sub>2</sub>)<sub>14</sub> *trans* conformation].  $^{29}\text{Si}$  CP/MAS NMR  $\delta = -57.8$  (T<sup>2</sup>),  $-67.1$  (T<sup>3</sup>).

**Polysiloxanyloctane (X1).** A mixture of 1 g ( $2.4 \times 10^{-3}$  mmol) of *n*-octyltrimethoxysilane, 5.2 g ( $2.2 \times 10^{-2}$  mmol) *n*-hexadecylamine and 5.5 g ( $2.2 \times 10^{-2}$  mmol) of TEOS were sol-gel processed in ethanol and water to yield a colorless swollen gel. After purification and drying 5.2 g of white powder was formed.  $^{13}\text{C}$  CP/MAS NMR:  $\delta = 13.2$  (SiCH<sub>2</sub> and CH<sub>3</sub>), 16.6 (OCH<sub>2</sub>CH<sub>3</sub>), 22.8 (SiCH<sub>2</sub>CH<sub>2</sub> and CH<sub>2</sub>CH<sub>3</sub>), 29.9 [(CH<sub>2</sub>)<sub>14</sub> *gauche* conformation], 32.0 [(CH<sub>2</sub>)<sub>14</sub> *trans* conformation], 59.3 (OCH<sub>2</sub>).  $^{29}\text{Si}$  CP/MAS NMR:  $\delta = -56.2$  (T<sup>2</sup>),  $-66.8$  (T<sup>3</sup>),  $-101.9$  (Q<sup>3</sup>),  $-109.5$  (Q<sup>4</sup>).

**Polysiloxanyloctane (X2).** A mixture of 1 g ( $2.4 \times 10^{-3}$  mmol) of *n*-octyltrimethoxysilane, 5.2 g ( $2.2 \times 10^{-2}$  mmol) *n*-hexadecylamine and 5.5 g ( $2.2 \times 10^{-2}$  mmol) of TMOS were sol-gel processed in ethanol and water to yield a colorless swollen gel. After purification and drying 4.2 g of white powder was formed.  $^{13}\text{C}$  CP/MAS NMR:  $\delta = 13.2$  (SiCH<sub>2</sub> and CH<sub>3</sub>), 16.6 (OCH<sub>2</sub>CH<sub>3</sub>), 22.8 (SiCH<sub>2</sub>CH<sub>2</sub> and CH<sub>2</sub>CH<sub>3</sub>), 29.9 [(CH<sub>2</sub>)<sub>14</sub> *gauche* conformation], 32.0 [(CH<sub>2</sub>)<sub>14</sub> *trans* conformation], 57.8 (OCH<sub>2</sub>).  $^{29}\text{Si}$  CP/MAS NMR:  $\delta = -57.2$  (T<sup>2</sup>),  $-67.8$  (T<sup>3</sup>),  $-101.5$  (Q<sup>3</sup>),  $-109.9$  (Q<sup>4</sup>).

**Polysiloxanyldodecane (X3).** A mixture of 1g ( $2.4 \times 10^{-3}$  mmol) of *n*-octyltrimethoxysilane, 5.2 g ( $2.2 \times 10^{-2}$  mmol) *n*-hexadecylamine and 5.2 g ( $2.2 \times 10^{-2}$  mmol) of MeSi(OMe)<sub>3</sub> were sol-gel processed in ethanol and water to yield a colorless swollen gel. After purification and drying 4.5 g of white powder was formed.  $^{13}\text{C}$  CP/MAS NMR:  $\delta = -3.6$  (CH<sub>3</sub>Si), 14.0 (SiCH<sub>2</sub> and CH<sub>3</sub>), 17.2 (OCH<sub>2</sub>CH<sub>3</sub>), 22.8 (SiCH<sub>2</sub>CH<sub>2</sub> and CH<sub>2</sub>CH<sub>3</sub>), 29.9 [(CH<sub>2</sub>)<sub>14</sub> *gauche* conformation], 32.8 9 [(CH<sub>2</sub>)<sub>14</sub> *trans* conformation], 57.4 (OCH<sub>2</sub>).  $^{29}\text{Si}$  CP/MAS NMR:  $\delta = -57.2$  (T<sup>2</sup>),  $-67.8$  (T<sup>3</sup>).

#### 4. Conclusion

The sol-gel process offers new hybrid materials **X0**, **X1**, **X2** and **X3**. A suitable pathway is the sol-gel processing of *n*-alkyl like *n*-octadecyltriethoxysilane with an aliphatic amine like *n*-hexadecylamine as template molecules and different cross-linkers such as Si(OEt)<sub>4</sub>, Si(OMe)<sub>4</sub> (Q<sup>0</sup>) and MeSi(OMe)<sub>3</sub> (T<sup>0</sup>) carried out in ethanol at room temperature. The structure of all xerogels (**X0–X3**) were determined by solid state  $^{13}\text{C}$  and  $^{29}\text{Si}$  NMR spectroscopy, infrared spectroscopy and SEM. Additionally, the mobility of the alkyl chains and the dynamic behavior of the polymer matrix depended strongly on the type of cross-linkers. At room temperature, pure *trans* was observed without cross-linker while trace amount

of *trans* was detected when  $Q^0$  cross-linkers were introduced. Both *trans* and *gauche* conformations in equal amounts were recorded when  $T^0$  cross-linkers were used.

## Acknowledgements

The project was supported by King Saud University, Deanship of Scientific Research, College of Science Research Center.

## References

1. Sander, L.C.; Sharpless, K.E.; Craft, N.E.; Wise, S.A. Development of engineered stationary phases for the separation of carotenoid isomers. *Anal. Chem.* **1994**, *66*, 1667–1674.
2. Sander, L.C.; Wise, S.A. Influence of stationary phase chemistry on shape recognition in liquid chromatography. *Anal. Chem.* **1995**, *67*, 3284–3292.
3. Karger, B.L.; Gant, J.R.; Hartkopf, A.; Weiner, P.H. Hydrophobic effects in reversed-phase liquid chromatography. *J. Chromatogr.* **1976**, *128*, 65–78.
4. Raitza, M.; Wegmann, J.; Bachmann, S.; Albert, K. Investigating the surface morphology of triacontyl phases with spin-diffusion solid-state NMR spectroscopy. *Angew. Chem.* **2000**, *39*, 3486–3489.
5. Pursch, M.; Sander, L.C.; Albert, K. Chain order and mobility of high-density C18 phases by solid-state NMR spectroscopy and liquid chromatography. *Anal. Chem.* **1996**, *68*, 4107–4113.
6. Lindner, E.; Al-Gharabli, S.; Warad, I.; Mayer, H.A.; Steinbrecher, S.; Plier, E.; Seiler, M.; Bertagnolli, H.Z. Supported organometallic complexes. XXXVI. Diaminediphosphine-ruthenium(II) interphase catalysts for the hydrogenation of  $\alpha,\beta$ -unsaturated ketones. *Z. Anorg. Allg. Chem.* **2003**, *629*, 161–171.
7. Lu, Z.L.; Lindner, E.; Mayer, H.A. Applications of sol-gel-processed interphase catalysts. *Chem. Rev.* **2002**, *102*, 3543–3578.
8. Rolison, D.R.; Dumn, B. Electrically conductive oxide aerogels: New materials in electrochemistry. *J. Mater. Chem.* **2001**, *11*, 963–980.
9. Salesch, T.H.; Bachmann, S.; Brugger, S.; Rabelo-Schaefer, R.; Albert, K.; Steinbrecher, S.; Plier, E.; Mehdi, A.; Reyé, C.; Corriu, R.; *et al.* New inorganic-organic hybrid materials for HPLC separation obtained by direct synthesis in the presence of a surfactant. *Adv. Funct. Mater.* **2002**, *12*, 134–142.
10. Tang, Q.; Wu, N.; Lee, M.L. Continuous-bed columns containing sol-gel bonded octadecylsilica for capillary liquid chromatography. *J. Microcolumn. Sep.* **2000**, *12*, 6–12.
11. Chan, M.A.; Lam, J.L.; Lo, D. Fiber optic oxygen sensor based on phosphorescence quenching of erythrosin B trapped in silica-gel glasses. *Anal. Chim. Acta* **2000**, *408*, 33–37.
12. Holder, E.; Oelkrug, D.; Egelhaaf, H.J.; Mayer, H.A.; Lindner, E. Synthesis, characterization, and luminescence spectroscopic accessibility studies of *tris*(2,2'-bipyridine)ruthenium(II)-labeled inorganic-organic hybrid polymers. *J. Fluoresc.* **2002**, *12*, 383–395.
13. Lindner, E.; Auer, F.; Schneller, T.; Mayer, H.A. Chemistry in interphases—A new approach to organometallic syntheses and catalysis. *Angew. Chem. Int. Ed.* **1999**, *38*, 2154–2174.

14. Matos, J.R.; Kruk, M.; Mercuri, L.P.; Jaroniec, M.; Zhao, L.; Kamiyama, T.; Terasaki, O.; Pinnavaia, T.J.; Liu, Y. Ordered mesoporous silica with large cage-like pores: Structural identification and pore connectivity design by controlling the synthesis temperature and time. *J. Am. Chem. Soc.* **2003**, *125*, 821–829.
15. Corriu, R.J.P.; Hoarau, C.; Mehdi, A.; Reyé, C. Study of the accessibility of phosphorus centers incorporated within ordered mesoporous organic-inorganic hybrid materials. *Chem. Commun.* **2000**, *1*, 71–72.
16. Jiao, J.; Sun, X.; Pinnavaia, T.J. Mesostructured silica for the reinforcement and toughening of rubbery and glassy epoxy polymers. *Polymer* **2009**, *50*, 983–989.
17. Thommes, M.; Kohn, R.; Froba, M. Characterization of mesoporous solids: Pore condensation and sorption hysteresis phenomena in mesoporous molecular sieves. *Stud. Surf. Sci. Catal.* **2002**, *142*, 1695–1702.
18. Sforca, M.L.; Yoshida, I.V.P.; Nunes, S.P. Organic-inorganic membranes prepared from polyether diamine and epoxy silane. *J. Membr. Sci.* **1999**, *159*, 197–207.
19. Pinho, R.O.; Radovanovic, E.; Torriani, L.I.; Yoshida, I.V.P. Hybrid materials derived from divinylbenzene and cyclic siloxane. *Eur. Polym. J.* **2004**, *40*, 615–622.
20. Schubert, U. Catalysts made of organic-inorganic hybrid materials. *New J. Chem.* **1994**, *18*, 1049–1058.
21. Arends, I.W.; Sheldon, R.A. Activities and stabilities of heterogeneous catalysts in selective liquid phase oxidations: Recent developments. *Appl. Catal. A* **2001**, *212*, 175–187.
22. Warad, I.; Al-Othman, Z.; Al-Resayes, S.; Al-Deyab, S.; Kenawy, E. Synthesis and characterization of novel inorganic-organic hybrid Ru(II) complexes and their application in selective hydrogenation. *Molecules* **2010**, *15*, 1028–1040.
23. Warad, I.; Siddiqui, M.; Al-Resayes, S.; Al-Warthan, A.; Mahfouz, R. Synthesis, characterization, crystal structure and chemical behavior of [1,1-bis(diphenylphosphinomethyl) ethene]ruthenium-(II) complex toward primary alkylamine addition. *Transition Met. Chem.* **2009**, *34*, 347–354.
24. Sayah, R.; Flochc, M.; Framery, E.; Dufaud, V. Immobilization of chiral cationic diphosphine rhodium complexes in nanopores of mesoporous silica and application in asymmetric hydrogenation. *J. Mol. Catal. A Chem.* **2010**, *315*, 51–59.
25. Kang, C.; Huang, J.; He, W.; Zhang, F. Periodic mesoporous silica-immobilized palladium(II) complex as an effective and reusable catalyst for water-medium carbon-carbon coupling reactions. *J. Organomet. Chem.* **2010**, *695*, 120–127.
26. Baiker, A.; Grunwaldt, J.D.; Muller, C.A.; Schmid, L. Catalytic materials by design. *Chimia* **1998**, *52*, 517–524.
27. Huesing, N.; Schubert, U. Aerogels-airy materials: Chemistry, structure, and properties. *Angew. Chem. Int. Ed.* **1998**, *37*, 22–45.
28. Pursch, M.; Brindle, R.; Ellwanger, A.; Sander, L.C.; Bell, C.M.; Haendel, H.; Albert, K. Stationary interphases with extended alkyl chains: A comparative study on chain order by solid-state NMR spectroscopy. *Solid State Nucl. Magn. Reson.* **1997**, *9*, 191–201.
29. Pursch, M.; Strohschein, S.; Haendel, H.; Albert, K. Temperature-dependent behaviour of C30 interphases. A solid-state NMR and LC-NMR study. *Anal. Chem.* **1996**, *68*, 386–393.

30. Pursch, M.; Sander, L.C.; Egelhaaf, H.J.; Raitza, M.S.; Wise, S.A.; Oelkrug, D.; Albert, K. Architecture and dynamics of C22 bonded interphases. *J. Am. Chem. Soc.* **1999**, *121*, 3201–3213.
31. Pines, A.; Gibby, M.G.; Waugh, J.S. Proton-enhanced NMR of dilute spins in solids. *J. Chem. Phys.* **1973**, *59*, 569–590.
32. Andrew, E.R. Narrowing of NMR spectra of solids by high-speed specimen rotation and the resolution of chemical shift and spin multiplet structures for solids. *Prog. Nucl. Magn. Reson. Spectrosc.* **1971**, *8*, 1–39.
33. Koenig, J.L.; Andreis, M. *Solid State NMR of Polymers*; Mathias L.J., Ed.; Plenum Press: New York, NY, USA, 1991.
34. Albert, K.; Bayer, E. Characterization of bonded phases by solid-state NMR spectroscopy. *J. Chromatogr.* **1991**, *544*, 345–370.
35. Fontes, M.M.; Oliva, G.; Cordeiro, L.C.; Batista, A. The crystal and molecular structure of bis[1,3-bis(diphenylphosphino)propane]dichlororuthenium(II). *J. Coord. Chem.* **1993**, *30*, 125–129.
36. Clauss, J.; Schmidt-Rohr, K.; Adam, A.; Boeffel, C.; Spiess, H.W. Stiff macromolecules with aliphatic side chains: Side-chain mobility, conformation, and organization from 2D solid-state NMR spectroscopy. *Macromolecules* **1992**, *25*, 5208–5214.
37. Maciel, G.E.; Sindorf, D.W. Silicon-29 NMR study of the surface of silica gel by cross polarization and magic-angle spinning. *J. Am. Chem. Soc.* **1980**, *102*, 7606–7607.
38. Mercier, L.; Pinnavaia, T. Direct synthesis of hybrid organic-inorganic nanoporous silica by a neutral amine assembly route: Structure-function control by stoichiometric, incorporation of organosiloxane molecules. *Chem. Mater.* **2000**, *12*, 188–196.

© 2012 by the authors; licensee MDPI, Basel, Switzerland. This article is an open access article distributed under the terms and conditions of the Creative Commons Attribution license (<http://creativecommons.org/licenses/by/3.0/>).